

# ARPES Study of the Metal-Insulator Transition in Bismuth Cobaltates

Z. Yusof,<sup>1</sup>[†] B.O. Wells,<sup>1</sup> T. Valla,<sup>2</sup> P.D. Johnson,<sup>2</sup> A.V. Fedorov,<sup>2</sup>[‡] Q. Li,<sup>3</sup> S.M. Loureiro,<sup>4</sup> and R.J. Cava,<sup>4</sup>

(1) Department of Physics, University of Connecticut,  
2152 Hillside Road U-46, Storrs, CT 06269-3046.

(2) Physics Department, Bldg. 510B, Brookhaven National Laboratory, Upton, NY 11973-5000.

(3) Division of Materials Sciences, Brookhaven National Laboratory, Upton, NY 11973-5000.

(4) Department of Chemistry and Materials Institute, Princeton University, Princeton, NJ 08544.

We present an angle-resolved photoemission spectroscopy (ARPES) study of a Mott-Hubbard-type bismuth cobaltate system across a metal-insulator transition. By varying the amount of Pb substitution, and by doping with Sr or Ba cation, a range of insulating to metallic properties is obtained. We observe a systematic change in the spectral weight of the coherent and incoherent parts, accompanied by an energy shift of the incoherent part. The band dispersion also shows the emergence of a weakly dispersing state at the Fermi energy with increasing conductivity. These changes correspond with the changes in the temperature-dependent resistivity behavior. We address the nature of the coherent-incoherent parts in relation to the peak-dip-hump feature seen in cuprates superconductors.

PACS numbers: PACS numbers: 71.30.+h, 79.60.-i, 71.28.+d

A central issue in condensed matter physics is the metal-insulator transition (MIT) in strongly-correlated electron systems, an issue in such areas as high- $T_c$  superconductors and CMR manganites. An important step to understand the nature of charge transport in such materials would be the ability to understand and predict the single-particle excitation spectrum - the spectral weight function - as measured by angle-resolved photoemission spectroscopy (ARPES). In most materials, there are a variety of complications to the ARPES spectra making a comparison to theory difficult. For example, in high- $T_c$  superconductors the most successful samples have multiple bands crossing the Fermi energy  $E_F$ , gaps at  $E_F$ , and anisotropic spectral lineshapes that differ strongly in different areas of the Brillouin zone. It would be helpful to study a compound with similar many-body physics and a similar MIT but with a simpler spectral function. Here we report on the ARPES-derived spectral functions of the layered oxide  $\text{Bi}_{2-x}\text{Pb}_x\text{M}_2\text{Co}_2\text{O}_8$ , with  $\text{M} = \text{Sr}, \text{Ba}, \text{Ca}$ . The spectral functions of these compounds appear to be simple enough to allow for a qualitative comparison to popular many-body models and indicate important trends as a function of temperature and doping.

Doping can cause a MIT in a  $d$ -band Mott insulator in two ways [1]. The first is charge doping to change the electron filling level. The second is iso-electronic chemical doping to alter the  $U/W$  ratio, where  $U$  is the on-site coulomb repulsion and  $W$  is the bandwidth. Both types of doping can be done in this family of cobalt oxides. Theoretically, models for this transition typically fall into one of two categories. The first starts from a description of the insulating state based upon the Hubbard Hamiltonian. In the Hubbard picture [2], reducing  $U/W$  causes the gap between the upper and lower Hubbard bands to close and a transition to a metal occurs when the bands overlap. The other category is the Brinkman-

Rice picture that starts from the metallic phase. Here, the quasiparticle (QP) band at  $E_F$  narrows and loses spectral weight as the transition is approached [3]. An approach that bridges these two approaches is the Dynamical Mean Field Theory (DMFT) [4]. As we show here, spectral functions for the DMFT are remarkably similar to those we have measured in these cobalt oxides.

The structure of the layered oxides of the type  $\text{Bi}_{2-x}\text{Pb}_x\text{M}_2\text{Co}_2\text{O}_8$  consist of rock salt layers of  $\text{Bi}(\text{Pb})\text{MO}_2$  interspersed with misfit hexagonal layers of  $\text{CoO}_2$  [6, 7, 8]. In general, samples with  $\text{M} = \text{Ba}$  are more conducting than those with  $\text{M} = \text{Sr}$ ; such doping is charge neutral and should be considered as primarily changing  $U/W$ . For a given  $\text{M}$  atom species, increasing the amount of Pb substituted for Bi increases the conductivity. It is believed that adding Pb increases the number of carriers, thus is primarily charge doping [8].

The Co ions appear to be in the low spin state as measured by susceptibility[6] and core level photoemission [9]. The Co oxidation state in a Pb-free  $\text{M} = \text{Sr}$  sample has been calculated to be 3.33 [10]. Thus it is unlikely that any of the compounds studied here are at half-filling, though many are strongly insulating. The more metallic samples are typically in-plane metallic and out-of-plane insulating at room temperature, metallic in all directions below some crossover temperature near 150K, and insulating in all directions at the lowest temperatures [6, 11]. Our previous ARPES work has shown that emergence of a sharp peak at  $E_F$  tied to a change in the  $c$ -axis resistivity from insulating ( $d\rho/dT < 0$ ) to metallic-like ( $d\rho/dT > 0$ ) [11]. For the  $\text{M} = \text{Sr}$  and no Pb doping, the insulating low temperature phase resistivity shows nearly activated behavior. In the same family, for Pb content over 0.4, the low temperature resistivity indicates variable range hopping [10].

Single crystals of  $\text{Bi}_{2-x}\text{Pb}_x\text{M}_2\text{Co}_2\text{O}_8$  with  $\text{M} = \text{Sr}$

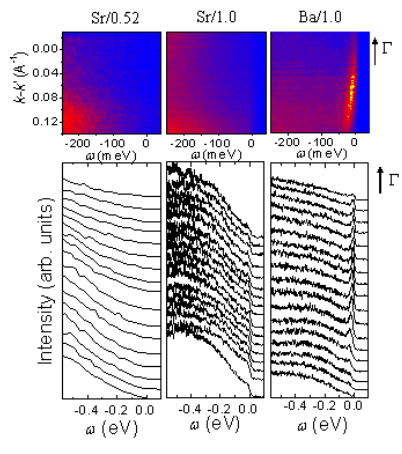


FIG. 1: (color) ARPES intensity for Sample  $Sr/0.52$  ( $T = 50K$ , left column),  $Sr/1.0$  ( $T = 40K$ , middle), and  $Ba/1.0$  ( $T = 30K$ , right). The top panels are the 2D intensity as a function of energy  $\omega$  and momentum  $k$  measured from  $k' = k_F$ , where  $k' = k_F$ , the Fermi wavevector for Sample  $Sr/1.0$ . The bottom panels are the corresponding EDCs over the same  $k$  range.

or Ba, were synthesized using the flux technique as described elsewhere [5]. For convenience we list the samples as  $M/x$  in order to describe both the cation and the Pb doping level. Thus  $Sr/0.52$  indicates  $Bi_{1.48}Pb_{0.52}Sr_2Co_2O_8$ . All ARPES measurements were performed at Beamline U13UB of the National Synchrotron Light Source, with photon energies of 15 eV and 21.2 eV. The end station includes a Scienta SES-200 hemispherical analyzer equipped for simultaneous collection of photoelectrons as a function of energy and angle. The crystals were cleaved *in situ* under vacuum with a base pressure of  $1 \times 10^{-10}$  Torr. The total energy resolution was  $\sim 15$  meV and momentum resolution better than  $0.02 \text{ \AA}^{-1}$ .

Fig. 1 shows the photoemission intensity near  $E_F$  along the rock salt cube-edge direction for a set of cobalt oxide samples. There is some variation in the dispersion in other directions but the lineshapes are essentially the same. The data is plotted both as two dimensional intensity maps as collected as well as energy dispersion curves (EDC's) at several  $k$  values. The left most panel is sample  $Sr/0.52$  which is the most insulating of those

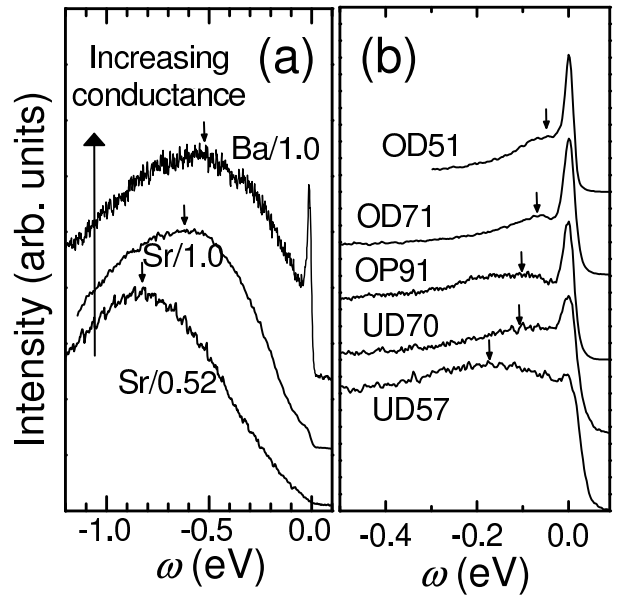


FIG. 2: (a) Broad EDC spectra of cobaltates, samples and temperatures as in Fig. 1. (b) EDC spectra of Bi2212 cuprates near the  $(\pi, 0)$  region in the superconducting state. UD69 is underdoped cuprate with  $T_c = 69K$ , OP91 is optimally-doped with  $T_c = 91K$ , and OD51 is overdoped with  $T_c = 51K$ . For comparison, each spectra have been normalized to the energy and intensity of the sharp peak. In both panels, the arrows point to the visual estimate of the location of the maximum broad peak.

examined here. Not surprisingly, there is no weight at  $E_F$  and a very broad feature with no discernible dispersion. The middle panel is sample  $Sr/1.0$ . This sample is charge doped with respect to  $Sr/0.52$  shown in the left most panel and is barely metallic, with details of the conductivity below. This sample has developed a barely discernible peak at  $E_F$  with slight dispersion. The right-most panel is  $Ba/1.0$ . This is the most metallic of those studied here. The change from the  $Sr/1.0$  in the middle panel involves substitution of Ba for Sr, and thus decreasing  $U/W$ . In the near  $E_F$  region we see a more intense peak with slightly greater dispersion. The existence of a sharp, slowly dispersion peak in the metallic samples that weakens as the insulator is approached is reminiscent of the Brinkman-Rice state approaching the insulator with increasing  $U/W$  [3].

Fig. 2a displays the EDC's of the same samples from Fig. 1 over a broader energy range and in a manner suitable for sample to sample comparison. The position and extent of the broad, incoherent part of the excitation is more easily seen here. The spectra are arranged in order of increasing room temperature conductance with the bottom spectra ( $Sr/0.52$ ) the least conducting,  $Sr/1.0$  in the middle, and  $Ba/1.0$  on top the most conducting. From the bottom spectrum to the middle, the predominant change is an increase in the number of carriers. From the middle spectrum to the top, the predominant

change is a decrease in  $U/W$ . The broad peak moves toward  $E_F$  with increasing conductivity regardless of the nature of the doping involved. The largest change is associated with adding charge carriers, presumably connected with a change in the chemical potential as in semiconductors. As mentioned above, changing the number of carriers in samples that are already basically conducting, there is a small change in the position of the incoherent states but a large increase in the spectral weight of the sharp, quasiparticle related peak at  $E_F$ .

There is a close connection between the spectral line-shape at  $E_F$  and the resistivity measurements. For  $Sr/0.52$ , the spectra consist of the broad, incoherent peak and a lack of any intensity at  $E_F$ . This corresponds with the insulating behavior in all directions of the temperature-dependent resistivity [5, 6]. In  $Sr/1.0$ , the spectra is still dominated by the broad incoherent peak, but a finite intensity develops at  $E_F$  with a weak coherent peak. As shown in Fig. 3(b) this sharp peak diminishes with increasing temperature, and is no longer detected at 130K. Fig. 3(a) shows that in-plane  $\rho_{ab}$  is metallic over the temperature range studied while  $\rho_c$  shows predominantly insulating behavior with a crossover to weakly metallic behavior below 120K. The downturn in  $\rho_c$  corresponds to the crossover temperature where the sharp peak in the ARPES spectra appears. Fig. 3(c) and (d) show similar behaviour, but with more pronounced peaks and a more pronounced turnover to metallic temperature dependence for  $\rho_c$ . These characteristics are consistent with that described in our earlier paper [11] which included measurements on a  $Ba/1.0$  type sample. In both metallic samples, the presence of the coherent, sharp peak in the spectra corresponds with the metallic behavior of  $\rho_c$ , whereas the metallic behavior of  $\rho_{ab}$  corresponds to the presence of a non-zero intensity in the spectra at the  $E_F$ .

Our previous paper established a connection between the temperature-dependent behavior of  $\rho_{ab}$  and  $\rho_c$  with the effective dimensionality of the system [11]. A 3D system is defined as having  $\rho_{ab}$  with similar temperature dependence as  $\rho_c$ , i.e.  $\rho_{ab}/\rho_c$  is constant. Hence, sample  $Ba/1.0$  is essentially 3D below 150K since both  $\rho_{ab}$  and  $\rho_c$  have similar behavior ( $d\rho/dT > 0$ ). On the other hand, above 200K, the sample shows 2D properties since  $\rho_{ab}$  and  $\rho_c$  have opposite behavior. The nature of the charge carriers in this 2D phase is unknown but appears to not be independent quasiparticles. In all cases the lowest temperature phase appears to be 3D in nature, whether metallic or insulating. This is reminiscent of high- $T_c$  superconductors such as  $La_{2-x}Sr_xCuO_4$  where measurement of the resistivity at low temperatures in the normal state induced by large magnetic fields, has shown  $\rho_{ab}$  and  $\rho_c$  to turn insulating for less than optimal doping [13]. Further, in those samples, for any doping  $\rho_{ab}$  and  $\rho_c$  are either both insulating or both metallic at lowest temperature.

We are not aware of a model that explicitly predicts a two-part MIT as a function of temperature. However, the

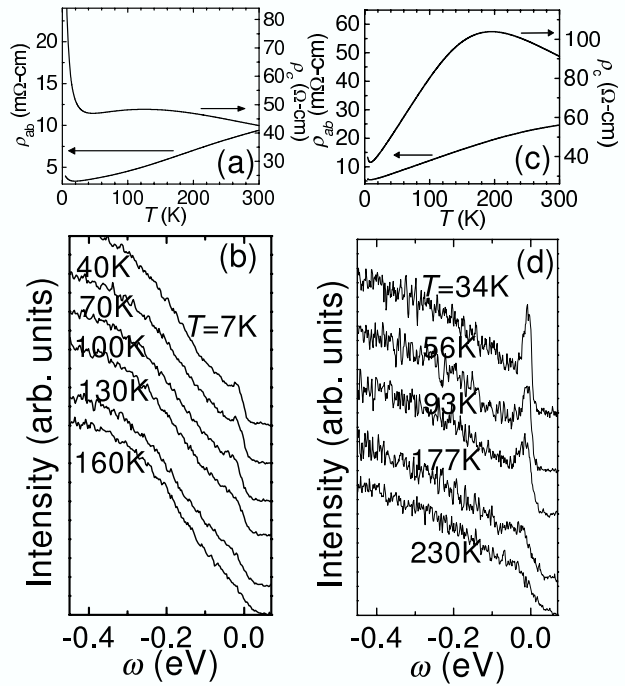


FIG. 3: Temperature dependent behavior of  $\rho_{ab}$  and  $\rho_c$  (top panels), and the ARPES spectra (bottom panels) for Samples  $Sr/1.0$  (Fig. (a) and (b)) and  $Ba/1.0$  (Fig. (c) and (d)).

ARPES spectra themselves have a strong resemblance to the spectral functions calculated within the frame work of the infinite-dimensional DMFT for a reasonable range of parameters [14, 15]. A comparison of Figs. 7-10 vs. 12-15 of Pruschke et al. [15] show the MIT as a function of carrier concentration. Pruschke et al. give the spectral functions in fig. 7 (for half filling and  $U=3$ ) and Fig. 12 (for hole doping of 0.03 and  $U=3$ ). The experimentally similar variation is going from the spectra of  $Sr/0.52$  to  $Sr/1.0$ . The differences are that our lower level of doping is not half filling and  $U$  in our samples is enough larger that there is a gap in the lesser-doped material. Aspects of our data which seem to match the calculation include the ubiquitous presence of a broad high energy excitation, a tendency for the broad peak to sharpen and move to lower energy with increasing conductivity, and the formation of a slowly dispersing sharp peak in the metallic state. The agreement for  $Sr/1.0$  extends to the region of low filling and high temperatures in which the calculated spectra have states at  $E_F$  but no QP peak. Further, changes between  $Sr/1.0$  and  $Ba/1.0$  are largely a function of changing  $U/W$ . While it is difficult to find a study that explicitly examines the spectral function as a function of  $U/W$  away from half filling, the trends can be seen in studies at half filling. Both Fig. 16 and Fig. 18 of reference [4] show the evolution of the spectral function as a function of  $U/W$ . The trends match our data in showing a substantial increase in the spectral weight of the sharp peak near  $E_F$  with decreasing  $U/W$  as well as significant lowering of the energy position of the broad,

incoherent peak. The most striking agreement between our data and the DMFT calculated spectral functions is for the temperature dependence of our most conducting sample,  $Sr/0.52$  as shown in Fig 3d here and Fig. 2 of [11], compared to Fig. 12 of Ref. [15].

The connection between the conductivity data and the DMFT calculations is less clear. The calculations indicate that the disappearance of the sharp peak in the density of states with increasing temperature corresponds to a transition to insulating isotropic resistivity at half filling (Figs. 12 and 14 of Ref. [15]). This is what we observe for  $\rho_c$  for the metallic phases [11]. The measured behavior of  $\rho_{ab}$ , i.e. that it remains metallic with no indication of the crossover, is not present in the DMFT calculations.

There are similarities between the spectral function for the cuprate superconductor Bi2212 and these cobaltates. Unlike the cobaltates, the cuprate spectral lineshapes are strongly anisotropic within the plane, at least for optimal or lesser doping. The cuprate spectra in the vicinity of the M-point are qualitatively similar to the cobaltates [16]. In Fig. 2b, spectra from Bi2212 at different doping levels: underdoped ( $T_c = 69K$ ), optimally doped ( $T_c = 91K$ ) [17], and overdoped ( $T_c = 51K$ ) [18]. The cuprate spectra are taken in the superconducting state near the M-point of the Brillouin zone. The spectra are arranged such that the top spectra comes from the most conducting compound (OD51) while the bottom spectra is from the least conducting (UD69) [19]. The two overall patterns that were observed in the cobaltates are repeated here for the cuprates. With increasing conductivity of the sample, the broad hump sharpens and shifts to lower energies, while the intensity of the sharp peak increases. In both cases the spectral evolution is consistent with that expected from DMFT calculations and it appears that the appearance of QP states corresponds with the emergence of isotropic electronic behavior.

A possible caveat to the above observation is that some literature has attributed the broad peak near the M-point in Bi2212 as being due to a second band of the bilayer CuO planes [20]. While there are few band calculations that explicitly consider charge doping, indications are that the splitting of the bilayer bands should be roughly independent of doping [21]. Since ARPES results show that the energy difference between the sharp peak and the broad peak clearly shrinks with doping, and the relative spectral weight of the broad peak continuously decreases, we conclude that this broad peak is not predominantly a second band. On the other hand, the evolution of this broad low energy peak is consistently predicted if this feature is predominantly the incoherent part of the excitation. In addition, at least one calculation that considers the effects of bilayer split bands explicitly predicts that this broad feature is predominantly due to the incoherent excitation [22].

The general picture put forward here concerning the relationship between the sharp quasiparticle peak and the broad incoherent peak it emerges from is extremely similar in spirit to a recent work concerning the evolution

of the cuprate compounds from Mott insulator to superconductor [23]. However, that work does not address the temperature evolution. Another system for which comparisons are naturally drawn are the compounds of the type  $Na_xCoO_2$ . For doping near  $x=0.35$  these are the precursors to the water intercalated superconductors with  $T_C = 5K$ . Those compounds consist of edge sharing  $CoO_6$  octahedra forming electronically active triangular sheets separated by Na layers and water in the hydrated versions. Thus those compounds have similar structure to the cobaltate compounds discussed here in many aspects. For heavily doped samples  $Na_{0.7}CoO_3$  the electronic structure near the Fermi level is very similar to that reported here for the most conducting compounds,  $Ba/1.0$  [24]. At low temperatures there is a predominantly circular Fermi surface, a broad peak near 0.7 eV about 0.6eV in width out of which a small, sharp peak emerges that is weakly dispersive. This was labelled as the quasiparticle peak similar to our own identification. The temperature dependence of that quasiparticle peak is also similar to what we detect, emerging below  $T = 120K$ . In that case it was reported that this temperature coincides to a change in the in-plane resistivity from T-linear at low temperature to a stronger dependence at high temperature. The out of plane resistivity was not reported. Interestingly, the lower doped  $Na_{0.3}CoO_3$  the equivalent quasiparticle peak has a much greater dispersion, perhaps indicating that  $U/W$  is much smaller for this latter compound [25]. Another group reporting on  $Na_{0.6}CoO_3$  found dispersion of the quasiparticle peak that was fairly broad, closer to that of  $Na_{0.3}CoO_3$  [26]. The exact behavior of this peak as a function of doping should prove very interesting.

In summary, we have shown ARPES results for the bismuth cobaltates across the MIT. The correlated insulators have broad, non-dispersing, incoherent spectra. The nominally metallic samples are more complex with at least two phases; (i) metallic behavior in the plane accompanied by the appearance of a Fermi edge in an otherwise broad spectral function and (ii) at lower temperatures a 3D electronic state occurs accompanied by the transfer of spectral weight to a sharp, slowly dispersing quasiparticle peak. As conductivity increases from sample to sample, either through increasing the number of holes or decreasing  $U/W$ , the broad incoherent part of the spectrum sharpens and shifts towards the Fermi energy and the sharp peak increases in intensity. The spectral function near the  $\Gamma M$  region of the Bi2212 superconducting compounds evolves similarly. Despite the prominence of a phase that is metallic in-plane and insulating out-of-plane, the zero temperature phase for all of the layered compounds appear to be 3D in nature.

We acknowledge valuable discussions with V. Perebeinos, A. Tsvelik, J. Tu, and R. Werner. Work supported in part by Dept. of Energy under contract number DE-AC02-98CH10886, DE-FG02-00ER45801, and DOE-BES W-31-109-ENG-38, and BOW acknowledges the support of a Cottrell Scholar Fellowship.

---

[†] Present address: High Energy Physics Div., Argonne National Laboratory, Argonne, IL 60439.

[‡] Present address: ALS, Lawrence Berkeley National Laboratory, Berkeley, CA 94720.

[1] A. Fujimori *et al.*, J. Elec. Spec. **117-118**, 277 (2001).

[2] J. Hubbard, Proc. R. Soc. London A **281**, 401 (1964).

[3] W.F. Brinkman and T.M. Rice, Phys. Rev. B **2**, 4302 (1970).

[4] A Georges *et al.*, Rev. Mod. Phys. **68**, 13 (1996).

[5] S.M. Loureiro *et al.*, Phys. Rev. B **63**, 94109 (2001).

[6] I. Tsukuda *et al.*, J. Phys. Soc. Jpn. **70**, 834 (2001).

[7] TEM studies in the group of R.J. Cava have confirmed a CoO hexagonal layer.

[8] T. Yamamoto *et al.*, Phys. Rev. B **65**, 184434 (2002).

[9] T. Mizokawa *et al.*, Phys. Rev. B **64**, 115104 (2001).

[10] Tsuyoshi Yamamoto *et al.*, Jpn. J. Appl. Phys. **39**, L747 (2000).

[11] T. Valla *et al.*, Nature **417**, 627 2002.

[12] Y. Watanabe *et al.*, Phys. Rev. B **43**, 3026 (1991).

[13] G.S. Boebinger *et al.*, Phys. Rev. Lett. **77**, 5417 (1997).

[14] M.J. Rozenberg *et al.*, Phys. Rev. Lett **83**, 3498 (1999).

[15] Pruschke *et al.*, Phys. Rev. B **47**, 3553 (1993).

[16] We note that the cuprate electronic structure is highly anisotropic. Only the cuprates spectra along the Cu-O bond direction ( $\Gamma$ M) show similar lineshapes with the cobaltates. This is the region that determines the  $c$ -axis transport of the cuprates.

[17] A.V. Fedorov *et al.*, Phys. Rev. Lett. **82**, 2179 (1999).

[18] Z.M. Yusof *et al.*, Phys. Rev. Lett. **88**, 167006 (2002).

[19] C. Kendziora *et al.*, Physica C **257**, 74 (1996).

[20] D.L. Feng *et al.*, Phys. Rev. B **65**, 220501 (2002); Y.-D. Chuang *et al.*, Phys. Rev. Lett. **87**, 117002 (2001); P. Bogdanov *et al.*, Phys. Rev. B **64**, 180505 (2001).

[21] I. Liechtenstein *et al.*, Phys. Rev. B **54**, 12505 (1996). See Fig. 5.

[22] M. Eschrig and M.R. Norman, Phys. Rev. Lett. **89**, 277005 (2002).

[23] K.M. Shen *et al.*, Phys. Rev. Lett. **93**, 267002 (2004).

[24] M.Z. Hasan *et al.*, Phys. Rev. Lett. **92**, 246402 (2004).

[25] M.Z. Hasan *et al.*, cond-mat/0501530 (2005).

[26] H.-B. Yang *et al.*, Phys. Rev. Lett. **92**, 246403 (2004).